Electronic Supplementary Material (ESI) for Physical Chemistry Chemical Physics.
This journal is © the Owner Societies 2021

Supplementary Information for "Theoretical study of laser-induced phenol photodissociation dynamics"

Xiaojuan Li,[1] Xinlu Cheng[2] and Hong Zhang,[1,2,*]

[1]College of Physical, Sichuan University, Chengdu 610065, China

[2]Key Laboratory of High Energy Density Physics and Technology of Ministry of Education, Sichuan

University, Chengdu 610065, China

*hongzhang@scu.edu.cn

S.1 Building up periodic Models

The periodic phenol molecular model is obtained by removing the surface of the adsorption model in which phenol is adsorbed on the surface of the two-dimensional g-C_3N_4 sheet, and the model phenol-over-graphene was accessed via replacing the 2D g-C_3N_4 sheet to monolayer graphene sheet.

For the adsorbed phenol molecule model: the upper and lower layers were deleted from the three-layer structure of mp-1193580 carbon nitride block structure in Material Project to obtain graphite phase carbon triazene with single-layer structure, g-C_3N_4. Then we sectioned the monolayer g-C_3N_4 structure with the crystal plane index (hkl) as 002, the thickness of the section as 1.5 (10.56 Å), the vacuum layer as 20 Å, and the direction as c along the z axis, consequently obtaining the periodic g-C_3N_4 monolithic layer structure stacked in the z direction. Furthermore, Castep module in Material Studio code is used to optimize the structure of monolithic layer g-C_3N_4. the specific setting details are: OTFG ultra-soft pseudopotential, generalized gradient approximation (GGA) in the form of perdew-Burke-ernzerhoff (PBE) functional, plane wave truncation energy set to 600 eV, The K point is set to 5x5x1 according to the Monkhorst-Pack Scheme lattice of vaspkit, only the optimized position does not optimize the lattice, and the energy

error criterion is set to 1.0 e^{-6} eV/atom. The obtained structure is used as an adsorbent for further adsorption process, and the unit structure of g-C_3N_4 nanosheet. Add dispersion (DFT+U) mode as TS.

Phenol molecules were constructed and optimized by Forcite module as the target adsorbate for further adsorption process. The adsorption position of g-C_3N_4 was predicted by Adsorption Locator module, and the adsorption pattern and adsorption position were traversed by COMPASS force field. the adsorption equilibrium configuration and corresponding energy were listed in Table S1.

Table S1 Physical adsorption position and corresponding adsorption energy

Item	Adsorption Location	Total energy	Adsorption energy	Rigid adsorption energy	Deformation energy	Benfen-forcite dEad/dNi
model1	atom1	-27.7374	-19.8817	-21.4609	1.5792	-19.8817
model2	atom1	-27.3185	-19.4627	-20.7752	1.3125	-19.4627
model3	atom1	-22.7675	-14.9118	-15.2594	0.3477	-14.9118
model4	Bounding box	-27.7374	-19.8817	-21.4609	1.5792	-19.8817
model5	Bounding box	-27.3185	-19.4627	-20.7751	1.3124	-19.4627
model6	Bounding box	-22.7675	-14.9118	-15.2592	0.3474	-14.9118
model7	Field values	-27.7374	-19.8817	-21.4609	1.5793	-19.8817
model8	Field values	-27.3185	-19.4627	-20.7749	1.3122	-19.4627
model9	Field values	-22.7675	-14.9118	-15.2592	0.3475	-14.9118
model10	atom2	-27.7374	-19.8817	-21.4609	1.5792	-19.8817
model11	atom2	-27.3185	-19.4627	-20.7752	1.3125	-19.4627
model12	atom2	-22.7675	-14.9118	-15.2594	0.3476	-14.9118
model13	atom3	-27.7374	-19.8817	-21.4609	1.5792	-19.8817
model14	atom3	-27.3133	-19.4575	-20.7699	1.3124	-19.4575
model15	atom3	-22.7675	-14.9118	-15.2593	0.3475	-14.9118
model16	atom4	-27.7374	-19.8817	-21.4609	1.5792	-19.8817

model17	atom4	-27.3133	-19.4575	-20.7700	1.3124	-19.4575
model18	atom4	-22.7675	-14.9118	-15.2594	0.3476	-14.9118
model19	atom5	-27.7374	-19.8817	-21.4609	1.5792	-19.8817
model20	atom5	-27.3185	-19.4627	-20.7752	1.3125	-19.4627
model21	atom5	-22.7675	-14.9118	-15.2593	0.3476	-14.9118
model22	atom6	-27.7374	-19.8817	-21.4608	1.5792	-19.8817
model23	atom6	-27.3185	-19.4627	-20.7752	1.3125	-19.4627
model24	atom6	-22.7675	-14.9118	-15.2593	0.3475	-14.9118
model25	**atom7**	**-27.7374**	**-19.8817**	**-21.4608**	**1.5791**	**-19.8817**
model26	atom7	-27.3185	-19.4627	-20.7750	1.3123	-19.4627
model27	atom7	-22.7675	-14.9118	-15.2594	0.3476	-14.9118
model28	atom8	-27.7374	-19.8817	-21.4609	1.5792	-19.8817
model29	atom8	-27.3185	-19.4627	-20.7752	1.3125	-19.4627
model30	atom8	-22.7675	-14.9118	-15.2595	0.3478	-14.9118
model31	all atom	-27.7374	-21.4609	-21.4609	0.0000	-21.4609
model32	all atom	-27.3185	-21.0419	-20.7751	-0.2668	-21.0419
model33	all atom	-22.7749	-16.4984	-15.2666	-1.2318	-16.4984
model34	6N of hole	-27.7374	-21.4609	-21.4609	0.0000	-21.4609
model35	6N of hole	-27.3185	-21.0419	-20.7751	-0.2668	-21.0419
model36	6N of hole	-22.7749	-16.4984	-15.2670	-1.2314	-16.4984
		-3.1081	-17.9267	-15.27807	-2.6486	-17.9267
		-2.7452	-17.5637	-14.9623	-2.6014	-17.5637
		-2.36511	-17.1837	-14.6380	-2.5457	-17.1837
		-1.6973	-16.5158	-13.9074	-2.6084	-16.5158
		-1.4623	-16.2809	-13.6867	-2.5942	-16.2809

As can be displayed in Stable1, the model25 with the lowest energy configuration is obtained, which takes atom No.7 as the target adsorption site. Subsequently, Castep module is used to optimize the structure to obtain the calculated ground state model modelI (pseudopotential is OTFG ultrasoft, truncation energy is 600 eV, K point is 5x5x1, energy deviation converges to 1.0 e^{-6} eV /atom, and force deviation converges to 1.0$e^{-1.74}$ ev/atom. The final structure energy is -4637.1412 eV, and the absorption energy is 0.5795 eV calculated via formula (S1), which is different from the single-layer g-C_3N_4 cell after structure optimization and phenol without g-C_3N_4 structure.

$$\Delta E_{adsorption} = E_{phenol\ on\ g-C_3N_4(002)} - E_{g-C_3N_4(002)} - E_{phenol\ molecule} \quad \text{(S1)}$$

Set the optimized model25 and phenol molecules in the same unit cell periodic structure without adsorbent as the initial photolysis structure, and name them as Model I and Model II respectively. The specific structures of them are shown in Figure S1, and the corresponding lattice parameters and coordinates are listed in Table S2 and S3.

Table S2 Unit cell parameter setting of Model I and II

Lattice vectors (Å)		
7.13450	0.00000	0.00000
-3.56725	6.17866	0.00000
0.00000	0.00000	20.0000
Lattice parameters-lengths (Å)		
a	b	c
7.1345	7.1345	20
Lattice parameters-angless (degrees)		
alpha	beta	gamma
90	90	120

Table S3 Atomic structure file of Model I

ID	Element	Symbol	x	y	z
1	C	C1	0.027325	1.280836	0.255000
2	C	C2	-1.175266	-0.745764	-0.366400
3	C	C3	1.227491	-0.755403	-0.303600
4	C	C4	-2.253824	1.263103	-0.069600
5	C	C5	0.016944	-2.708168	-0.314400
6	C	C6	2.302018	1.256986	-0.048200
7	C	C7	-0.493921	-1.193964	3.439600
8	C	C8	-0.305963	0.098920	3.934800
9	C	C9	0.981208	0.645670	3.951000
10	C	C10	2.066401	-0.077419	3.457800
11	C	C11	1.876195	-1.367522	2.936600

12	C	C12	0.588953	-1.929471	2.951400
13	N	N13	-1.170379	1.889001	0.450600
14	N	N14	-1.166098	-2.080663	-0.461800
15	N	N15	2.345966	-0.029163	-0.385200
16	N	N16	-2.274015	0.010195	-0.514000
17	N	N17	1.206872	1.911306	0.391400
18	N	N18	1.207692	-2.091538	-0.397000
19	N	N19	0.024115	-0.071055	-0.119400
20	N	N20	-3.547452	2.016652	-0.136400
21	O	O21	2.963386	-2.016714	2.435400
22	H	H22	-1.491860	-1.636418	3.424400
23	H	H23	-1.152079	0.674092	4.311600
24	H	H24	1.140450	1.653162	4.338800
25	H	H25	3.070974	0.347982	3.457200
26	H	H26	0.442624	-2.948209	2.587400
27	H	H27	2.693452	-2.744127	1.825600

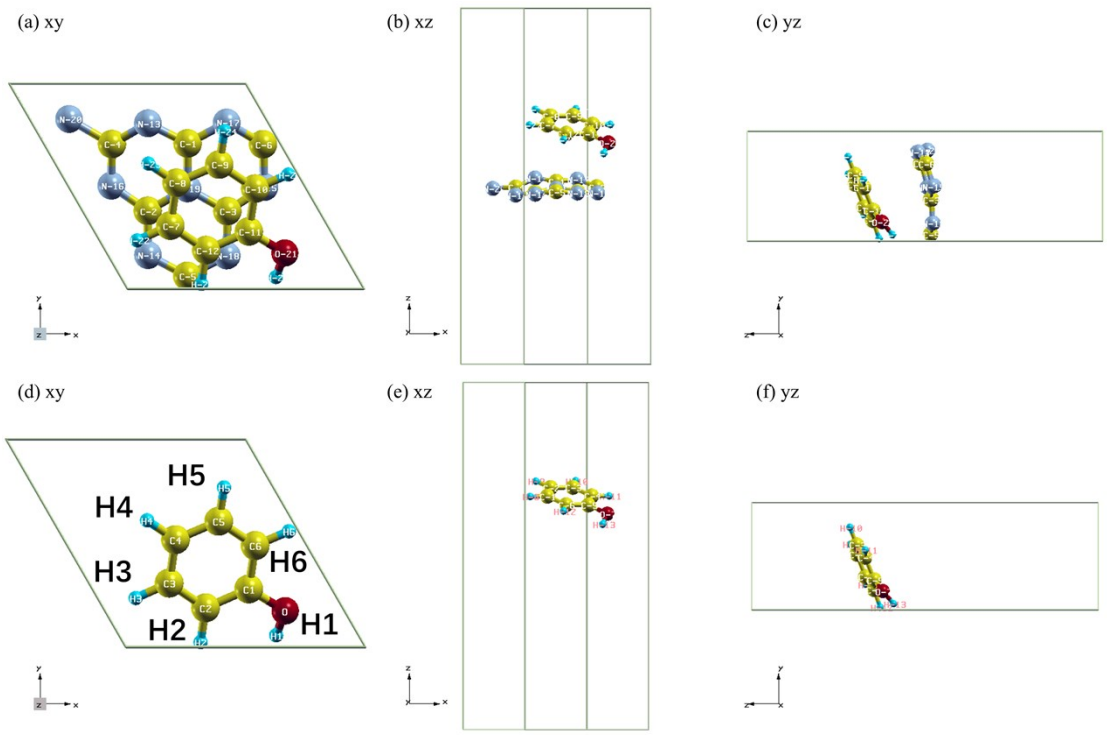

Figure S1The top (a: plane_z), front (b: plane_y) and side (c: plane_x) view of the schematic diagram of Graphical representation of Model I: Physical adsorption of phenol molecule on the surface monolayer g-C_3N_4 sheet; and the corresponding vies (d, e and f) of Model II: An isolated phenol molecule in the same lattice.

Table S4 Initial bond length of the isolated phenol molecule in Model II

Bond	O-H1	C2-H2	C3-H3	C4-H4	C5-H5	C6-H6

(Å)	0.987	1.092	1.092	1.090	1.091	1.091
C1-C2	C2-C3	C3-C4	C4-C5	C5-C6	C6-C1	CO
1.405	1.397	1.397	1.399	1.394	1.404	1.362

All atoms of a phenol molecule were stamped as following in Figure S1(d): (1) setting the H atom of the phenolic hydroxyl as H1; (2) setting the C atom connecting to H1 as C1; (3) whereafter sorting C atoms and corresponding H atoms in turn clockwise as C2-6, H2-6. The initial bond length was listed in Table S4.

S.2 Detail Sets to Keep Numerical Stability in Dynamics Procedure

S.2.1 Spacing

As we all known, the spacing between the points of the mesh is the key parameter of a real-space calculation. The convergence with respect to the grid spacing must be performed for all quantities of interest in a real-life calculation. We have carried out several sets of experiments to test the validity of the parameter applied in this paper. In this section, we convert the spacing parameter to converge a quantity of interest, such as the total energy, s_eigen and p_eigen.

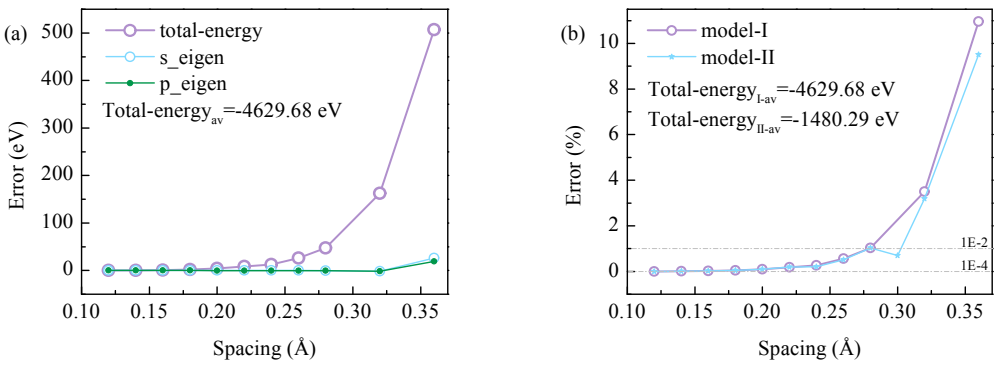

Figure S2 Convergence with spacing of model-I and model-II

The results, for the two different models, are shown in the Figure S3. Considering that the smallest spacing provides the most accurate result, we are actually focusing the difference between the total-energy for a given spacing and that for a spacing of 0.12 Å and plot the ratio of the differences in the Figure S3. As we can see from this picture, the total energy is converged[1] to within 2 eV (about 0.04% of the average of total energies) for a spacing of 0.18 Å. However, as we

are usually not interested in total energies, but in energy differences, we prefer to the spacing = 0.2 Å (about 0.1% of the average of the total energies) for the whole calculations instead of 0.18 Å, with cutoff energy being about 69 Ry, saving about 1/3 machine hours being and without compromising the results.

S.2.2 Time step

Furthermore, the critical way to keep numerical stability in dynamics procedure is to adopt an adequate time step[2]. For the whole atomic simulation of molecular system, the step size should be less than 10% of the reciprocating period of the bond with the highest vibration frequency in the system. The TDDFT evolution operator to evolve the wave function of the ground state electronic structure of each macroscopic position in Octopus code is:

$$e^{-iH\Delta t} \approx \sum_{n=0}^{4} \frac{(i\Delta t)^n}{n!} H^n \tag{1}$$

$$\Delta t < \sqrt{\frac{2}{9} m (\Delta x)^2} \approx 0.2\ a.u. \tag{2}$$

where H is the Kohn-Sham single-particle Hamiltonian appearing. The algorithm (1) is stable if Δt provided satisfied as equation (2). Δx is the spacing between the points of the mesh. According to such limiters, time step should be less than 0.067 a.u(≈ 0.0016 fs) for spacing = 0.2 Å. We use a somewhat smaller value in the calculations below, Δt = 0.001 fs (≈ 0.041 au) at first. Then we found that even if the time interval is increased by an order of magnitude (which can greatly reduce the consumption of computing resources), we can still get the same result. And in this situation, for the total time as 50 fs, our time dependent max steps will be 5000, which is sufficient to make sure the stability of this time propagation process while dt is 0.01 fs. Therefore, after measuring the target and consumption, we choose to set the time interval as 0.01 fs, at this time, the propagation process is still stable and the total energy of the system is still conserved normally.

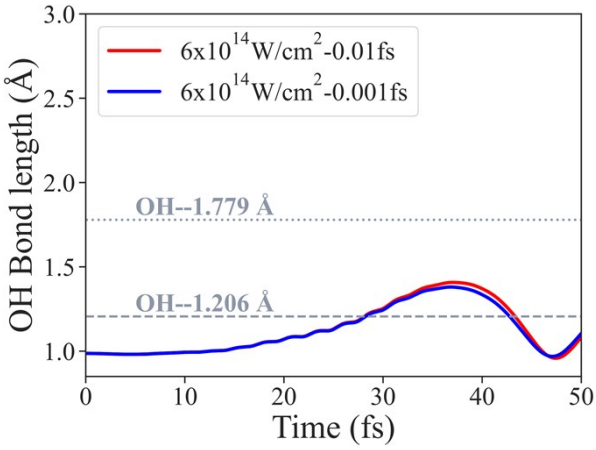

Figure S3 Time evolution of the OH bond lengths of the phenol under the pulse laser with intensity being 6×10^{14}W/cm^2, wavelength being 800 nm and duration lasting for 40 fs with differ time interval.

The light gray short dashed line locates the bond length when OH expresses the 'broken state' in the XCRYSDEN code and the dotted line show the actual fracture.

S.3 laser set

People usually utilize intensity to describe the strength of laser field rather than the electric-field amplitude. The relationship between instantaneous electric field (*I(t)*) and intensity(*E(t)*) in atomic units can be described as:

$$I(t) = \frac{c}{8\pi}E^2(t) \tag{3}$$

To describe the laser intensity in W/cm^2, we have to perform a series of conversions. The dimensions of intensities are [W]/(L^{2}T), where [W] are the dimensions of energy. The relevant conversion factors are as follows:

$$\text{Hartree}/(a_0^2\text{atomictime}) = 6.364086\times10^{15}\ \text{W/cm}^2 \tag{4}$$

$$\text{eV}/(\text{Å}^2(\hbar/eV)) = 2.4341348\times10^{12}\ \text{W/cm}^2 \tag{5}$$

$$I_0 = 3.51\times10^{16}\ \text{W/cm}^2(E_0^2) \quad \text{(a.u.)} \tag{6}$$

$$1\text{E}_0\text{(a.u.)}=1\ \text{Hartree/bohr/e} = 51.423\ \text{(V/Å)} \tag{7}$$

According to these equations, we can get the laser intensities we used in this paper.

Table S5 Intensity of the applied lasers

4	5	6	7	8	9	$\times10^{14}$ W/cm^2
5.49	6.14	6.72	7.26	7.76	8.23	V/Å

Figure S4 shows the waveform of the laser pulses applied to the isolated phenol model with a wavelength of 800 nm, pulse duration of 40 fs, and various laser strength (and thereinto, the laser power densities (laser intensities) I are 4×10^{14}W/cm^2, 5×10^{14}W/cm^2, 6×10^{14}W/cm^2, 7×10^{14}W/cm^2, 8×10^{14}W/cm^2 and 9×10^{14}W/cm^2, where the corresponding intensities of the instantaneous electric field E: are 5.49 V/Å, 6.14 V/Å, 6.72 V/Å, 7.26 V/Å, 7.76 V/Å, and 8.23 V/Å respectively).

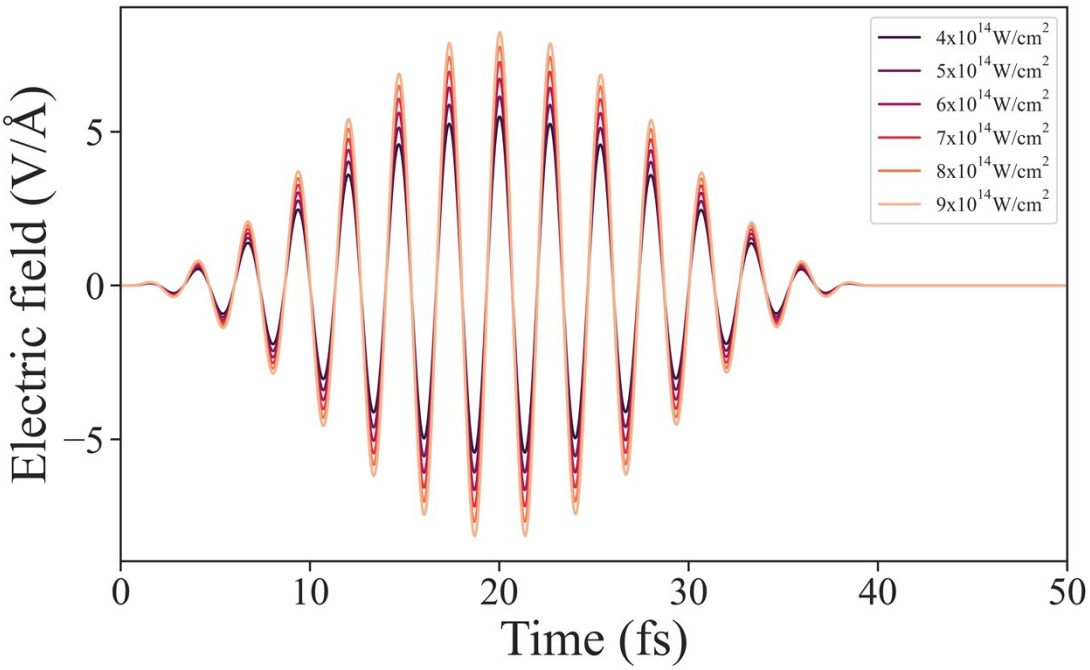

Figure S4 Waveform of the incident laser pulse.

S.4 Time evolution of other bond lengths

S.4.1 O-H1

As can be seen in Figure S.5, the phenol molecule has a tendency to rotate to the positive direction of the z axis. When there is no laser, the molecule is approximately parallel to the xz plane after rotating 200 fs. In the presence of laser, the phenol molecule can rotate to the same position in less than100 fs, i.e., when there is an 800 nm- 40 fs- 4×10^{14}W/cm^2 laser, the rotation speed of the molecule is twice as fast.

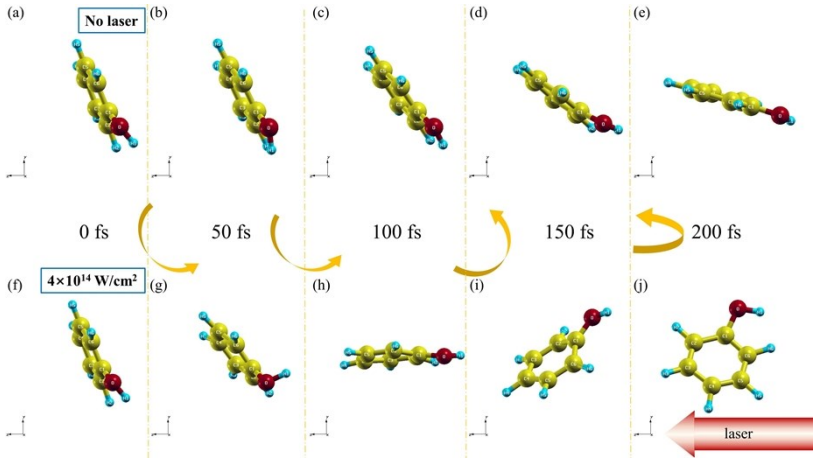

Figure S4 Time evolution of phenol molecule under 800 nm-40 fs laser with (a-e) 0×10^{14}W/cm^2 and (f-j) 4×10^{14}W/cm^2

S.4.2 C-Hs

As similar to the O-H bond, we marked the phenomenon that the C-H bond length exceeds the short-dashed line (1.206 Å) while it presented a 'broken state' in the visible code yet regard the length of 2.184 Å, when the ELF patterns prove the bonds being fracture, as reliable predictors of the actual decomposition. As can be seen in Figure S6, we can find when the laser intensity is below 7×10^{14} W/cm^2, all the carbon-hydrogen bonds (C-H) of phenol maintain their structures and stay tight to the ring. While the laser intensity reaches 7×10^{14} W/cm^2, the C2-H2 (occupying the ortho-position of the C1 attached to the hydroxyl group), C4-H4 (occupying the para-position), and C5-H5 bond (occupying the anti-meta-position) all start to oscillate and the C5-H5 bond presented the most violent vibration. Although they exhibit fracture graphic in the final state at 50 fs as shown in Figure S5(d), we still believe the bonds C2-H2, C4-H4, and C5-H5 of an isolated phenol still have not turned fracture while the laser is no more than 7×10^{14} W/cm^2. The ELF picture in Figure 3 (d-f) can support this point. While the laser intensity reaches 8×10^{14} W/cm^2, the bond C5-H5 breaks smoothly, and C2-H2 and C4-H4 remain oscillating and thereinto, the bond C4-H4 oscillated more violently. While the laser intensity reaches 9×10^{14} W/cm^2, the bonds C5-H5, C2-H2, and C4-H4 all break smoothly and the C3-H3(occupying the meta-position) started to oscillate. As can be seen in Figure 4 (g-i), for the intensity being 9×10^{14} W/cm^2, the local electrons over the C5-H5 bond turned to disperse between 33 and 33.5 fs. We can only get a series of ELF documents at time intervals of

0.5 fs owing to the limitation of technical resources, and meanwhile, the bond of O-H was between 2.141 Å and 2.228 Å, so we propose the real decomposition bond of C-H as 2.184 Å. The timings when the C2-H2 and C4-H4 get through this length limit are at 40.82 fs and 35.14 fs, which informs the stability order of C-Hs as C5-H5 < C4-H4 < C2-H2. Furthermore, we believe it is also the excitation of electrons involved in the C-H bond of the phenol molecule that promotes the decomposition just as the H1 atom left the O-H1 bond. Among all the Figures of the time evolution of the C_iH_i (i= 2, 3, 4, 5) bond lengths, we find the image of C6-H6 (occupying the anti-ortho-position) is a very unique existence with a sudden change in the bond length occurring between 31.45 fs to 33.51 fs. Through the dynamic graphs we find that the H6 atom linked to C6 has been moving in the positive direction of x over time, reaching the box boundary at 31.44 fs, thus jumping to the other side, causing the bond length to jump from 1.223 Å (31.44 fs) to 6.005 Å (31.45 fs). With the passage of time and the concussion of the bond, the H6 atom returned to its original position at 33.51 fs and stayed there till the final propagation time (as can been seen in Figure S6(e-f)). Moreover, from the Figure 3(g-i), it can be seen that the electrons are still located around the bond C6-H6, which indicated its integrity. Therefore, we can conclude it is only because of the limitation of the periodic boundary that the position of the H6 atom transitions to the other side of the corresponding lattice. After modulating it, we can get a spectrum similar to C3-H3, that means, C6-H6 also does not really fracture in the whole process, even if the laser intensity has been reached 9×10^{14}W/cm^2. This phenomenon can also be seen in Figure S5(f) and Figure 3(i), which also proves the importance of periodic boundaries usage in the analysis of single-molecule decomposition dynamics. You can see the full dynamics mentioned in several separated gif files in our supporting materials.

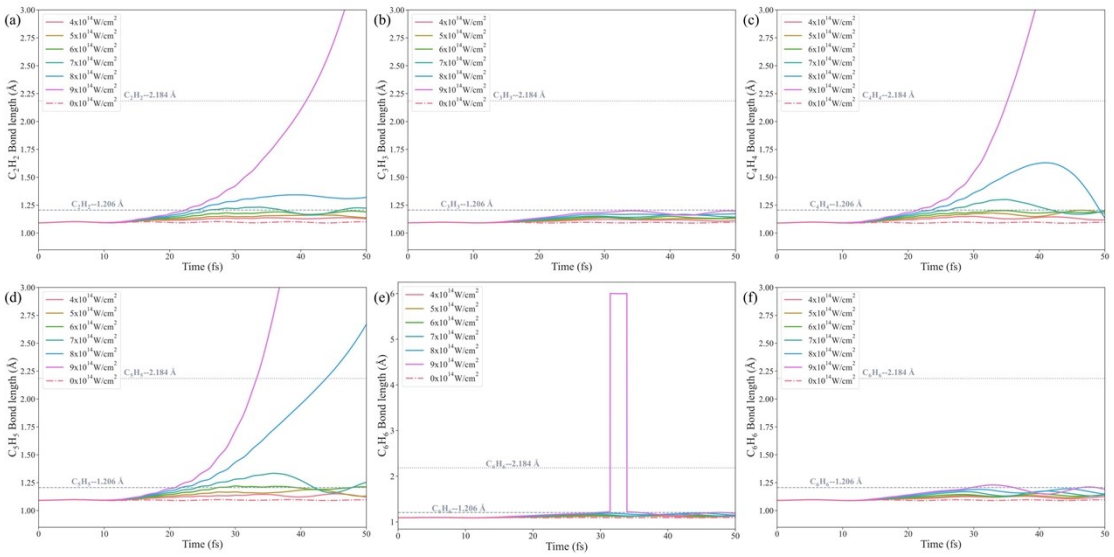

Figure S5 Time evolution of the C_iH_i (i= 2, 3, 4, 5,6) bond lengths of the phenol under the pulse laser with different intensities. Intensities are colored by order. The light gray dotted line locates the bond length when C-H expresses the fracture in the XCRYSDEN code.

(a) C2-H2 (b) C3-H3 (c) C4-H4 (d) C5-H5 (e) C6-H6 and (f) the modification of C6-H6

Table S6 Final bond length of C-Hs under different laser (50 fs)

Bonds	C2-H2	C3-H3	C4-H4	C5-H5	C6-H6
r_0 (Å)	1.092	1.092	1.090	1.091	1.091
0×10^{14} W/cm^2	0.89%	0.28%	0.49%	0.48%	0.51%
4×10^{14} W/cm^2	3.34%	1.70%	2.60%	2.71%	2.95%
5×10^{14} W/cm^2	4.15%	3.49%	7.69%	3.55%	4.64%
6×10^{14} W/cm^2	8.93%	4.45%	9.44%	11.03%	4.86%
7×10^{14} W/cm^2	12.05%	4.70%	10.22%	14.81%	4.41%
8×10^{14} W/cm^2	21.03%	7.42%	4.06%	144.64%	5.23%
9×10^{14} W/cm^2	239.26%	9.53%	406.45%	657.39%	8.66%

r_0, the initial length of C-H bond; r, the final length of C-Hs bonds under laser with different intensities are not listed; $\Delta r\%$, the ratio of variation difference to initial value: $\Delta r=(r-r_0)/r$

S.4.3 C-Cs &C-O

As can be seen in Figure S5, the 'broken state' of the C1-C2, C3-C4, and C6-C1 bonds could be noticed at final time pictures, yet no real fracture of any C-C bond has occurred under the current laser intensity proven from the ELF patterns in Figure 3. Besides, it can also be confirmed that there are no C-C bonds with a bond length longer than 3 Å in the bond length change diagram of Figure

S7. The time when the 'breaking' of C1-C2, C3-C4, and C6-C1 can be detected are at 37.91 fs, 31.75 fs, and 37.91 fs, when their bond length got through the length limit of 1.625 Å with the laser intensity being 9×10^{14}W/cm^2. The 'breaking' of the C-O bond has not been observed in all the processes. Consequently, it can be inferred that the stable order of different types of bonds in an isolated phenol is: O-H < C-H. The Time evolution of every bond while the intensity is 9×10^{14}W/cm^2 is plotted in Figure 4(d), illustrating only the O-H, and C5-H5, C4-H4 and C2-H2 bonds actually fracture. We noticed that the C-O bond length in all free radicals is shorter than that of the molecular state, but the bond length is slightly longer than that of p-benzoquinone and cyclohexanone with true C=O double bonds. Because after the formation of free radicals, the unbonded single-occupied p orbital of the O atom is conjugated with the benzene ring and the O atom has a stronger ability to attract electrons than the C atom. The detailed messages of change value of bonds' lengths are listed in Table S7. All in all, setting the O-H fracture as the signal of success decomposition, the threshold intensity of the laser field for phenol photodissociation should be 7×10^{14}W/cm^2, yet if C5-H5 fracture is used as a signal, the threshold intensity should be 8×10^{14}W/cm^2 and at least 9×10^{14}W/cm^2 for other bonds.

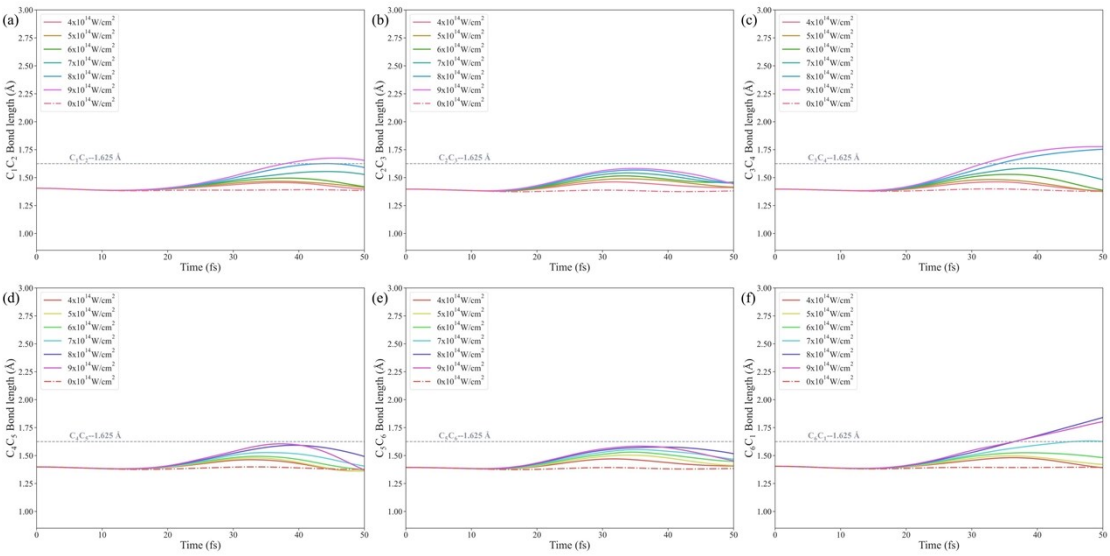

Figure S6 Time evolution of the Ci-Cj (i=1, 2, 3, 4, 5, 6; j = 2, 3, 4, 5, 6, 1) bond lengths of the phenol under the pulse laser with different intensities. Intensities are colored by order. The light gray dotted line locates the bond length when C-C expresses the fracture in the XCRYSDEN code.

Table S7 The change value of the final bond length of C-Cs/C-O under different laser (50 fs)

Bonds	C1-C2	C2-C3	C3-C4	C4-C5	C5-C6	C6-C1	CO
r_0 (Å)	1.405	1.397	1.397	1.399	1.394	1.404	1.362

0×10^{14} W/cm^2	-1.45%	-1.16%	-1.42%	-1.44%	-0.69%	-0.71%	-0.86%
4×10^{14} W/cm^2	-0.56%	0.95%	-1.17%	-2.54%	0.91%	-0.87%	2.81%
5×10^{14} W/cm^2	0.57%	1.26%	-1.63%	-2.67%	1.31%	1.16%	6.94%
6×10^{14} W/cm^2	0.96%	4.48%	-0.73%	-1.80%	3.86%	5.48%	9.75%
7×10^{14} W/cm^2	8.76%	3.80%	6.07%	0.50%	5.22%	15.83%	-6.16%
8×10^{14} W/cm^2	13.21%	3.82%	25.54%	6.70%	8.78%	31.08%	-6.90%
9×10^{14} W/cm^2	17.75%	3.33%	27.13%	-1.97%	4.19%	28.44%	-2.91%

r_0, the initial length of CCs/CO bonds; r, the final length of C-Cs/C-O bonds under laser with different intensities are not listed; $\Delta r\%$, the ratio of variation difference to initial value: $\Delta r=(r-r_0)/r$

S.5 Mechanism analysis

S.5.1 Pearson correlation analysis (r) and corresponding significance level P value

Table S8 Final energies and the number of bonds in this paper

	intensity	wavelength	duration	Total	Total -cumulant	Kinetic(ions)	Ion-Ion	Ion-Ion -cumulant	Ion-Ion	bonds
	4	800	40	-1104.97	357.66	1.85	2877.03	-210.59	210.59	0
	5	800	40	-929.77	532.86	3.03	2789.67	-297.95	297.95	0
	6	800	40	-780.08	682.55	4.61	2662.14	-425.48	425.48	0
	7	800	40	-668.39	794.24	15.50	2382.20	-705.42	705.42	1
	8	800	40	-471.75	990.88	18.83	2151.43	-936.19	936.19	2
intensity	9	800	40	-187.49	1275.15	37.05	1797.21	-1290.41	1290.41	4
	7	400	40	-729.83	732.80	44.37	1372.47	-1715.16	1715.16	4
	7	600	40	-724.45	738.18	18.45	2268.92	-818.70	818.70	1
	7	800	40	-668.39	794.24	15.50	2382.20	-705.42	705.42	1
wavelength	7	1000	40	-490.97	971.66	11.89	2477.47	-610.15	610.15	1
	7	800	10	-1223.42	239.22	2.06	2801.44	-286.18	286.18	0
	7	800	20	-1011.23	451.40	3.91	2686.44	-401.18	401.18	0
	7	800	30	-813.01	649.63	5.07	2609.88	-477.74	477.74	0
duration1	7	800	40	-668.39	794.24	15.50	2382.20	-705.42	705.42	1
	9	800	10	-1117.63	345.01	3.52	2660.48	-427.14	427.14	0
	9	800	20	-822.99	639.64	14.17	2455.65	-631.97	631.97	1
	9	800	30	-537.69	924.94	14.61	2352.57	-735.05	735.05	1
duration2	9	800	40	-187.49	1275.15	37.05	1797.21	-1290.41	1290.41	4

$$\rho_{X,Y} = \frac{cov(X,Y)}{\sigma_X \sigma_Y} = \frac{E((X-\mu_X)(Y-\mu_Y))}{\sigma_X \sigma_Y} = \frac{E(XY) - E(X)E(Y)}{\sqrt{E(X^2) - E^2(X)}\sqrt{E(Y^2) - E^2(Y)}}$$

X is the variable in line and *Y* is variable in the second column. r is the Pearson product-moment correlation coefficient, i.e., $\rho_{X,Y}$.

1. Intensity

Data from the 'intensity' lines in Table S8

Table S9 The Pearson correlation coefficient (r) and actual measuring significance level P-value (P) for intensity and Kinetic energy release/the number of broken bonds

r	Intensity ($\times 10^{14}$ W/cm^2)	E_{Total}	E_{Kin}	$E_{Ion\text{-}Ion}$	number
intensity	1.000	0.989	0.928	-0.977	0.901
E_{Total}	0.989	1.000	0.956	-0.987	0.940
E_{Kin}	0.928	0.956	1.000	-0.982	0.989
$E_{Ion\text{-}Ion}$	-0.977	-0.987	-0.982	1.000	-0.971
number	0.901	0.940	0.989	-0.971	1.000
P	Intensity ($\times 10^{14}$ W/cm^2)	E_{Total}	E_{Kin}	$E_{Ion\text{-}Ion}$	number
intensity	0.000	0.000	0.008	0.001	0.014
E_{Total}	0.000	0.000	0.003	0.000	0.005
E_{Kin}	0.008	0.003	0.000	0.001	0.000
$E_{Ion\text{-}Ion}$	0.001	0.000	0.001	0.000	0.001
number	0.014	0.005	0.000	0.001	0.000

where E_{Total} is total energy of system change; E_{Kin} is Kinetic energy release; $E_{Ion\text{-}Ion}$ is the Coulomb repulsive energy; number is the number of broken bonds at the end of the 50-fs photodissociation processes.

2. Wavelength

Data from the 'wavelength' lines in Table S8

Table S10 The Pearson correlation coefficient (r) and actual measuring significance level P-value (P) for wavelength as single variable

r	Wavelength (nm)	E_{Total}	E_{Kin}	$E_{Ion\text{-}Ion}$	number
wavelength	1.000	0.892	-0.876	0.869	-0.775
E_{Total}	0.892	1.000	-0.605	0.590	-0.456
E_{Kin}	-0.876	-0.605	1.000	-1.000	0.983
$E_{Ion\text{-}Ion}$	0.869	0.590	-1.000	1.000	-0.986
number	-0.775	-0.456	0.983	-0.986	1.000
P	Wavelength (nm)	E_{Total}	E_{Kin}	$E_{Ion\text{-}Ion}$	bonds
wavelength	0.000	0.108	0.124	0.131	0.225
E_{Total}	0.108	0.000	0.395	0.410	0.544

E_{Kin}	0.124	0.395	0.000	0.000	0.017
$E_{Ion\text{-}Ion}$	0.131	0.410	0.000	0.000	0.014
number	0.225	0.544	0.017	0.014	0.000

3. Duration

Data from the 'duration' lines in Table S8

Table S11 The Pearson correlation coefficient (r) and actual measuring significance level P-value (P) for wavelength as single variable

laser 7×10^{14}W/cm^2-800 nm

r	duration (fs)	E_{Total}	E_{Kin}	$E_{Ion\text{-}Ion}$	number
duration	1.000	0.997	0.887	-0.973	0.775
E_{Total}	0.997	1.000	0.846	-0.952	0.720
E_{Kin}	0.887	0.846	1.000	-0.968	0.979
$E_{Ion\text{-}Ion}$	-0.973	-0.952	-0.968	1.000	-0.896
number	0.775	0.720	0.979	-0.896	1.000
P	duration (fs)	E_{Total}	E_{Kin}	$E_{Ion\text{-}Ion}$	bonds
duration (fs)	0.000	0.003	0.113	0.027	0.225
E_{Total}	0.003	0.000	0.154	0.048	0.280
E_{Kin}	0.113	0.154	0.000	0.032	0.021
$E_{Ion\text{-}Ion}$	0.027	0.048	0.032	0.000	0.104
number	0.225	0.280	0.021	0.104	0.000

laser 9×10^{14}W/cm^2-800 nm

r	duration (fs)	E_{Total}	E_{Kin}	$E_{Ion\text{-}Ion}$	number
duration	1.000	0.999	0.925	-0.942	0.894
E_{Total}	0.999	1.000	0.940	-0.957	0.914
E_{Kin}	0.925	0.940	1.000	-0.994	0.995
$E_{Ion\text{-}Ion}$	-0.942	-0.957	-0.994	1.000	-0.992
number	0.894	0.914	0.995	-0.992	1.000
P	duration (fs)	E_{Total}	E_{Kin}	$E_{Ion\text{-}Ion}$	bonds
duration (fs)	0.000	0.001	0.075	0.058	0.106
E_{Total}	0.001	0.000	0.060	0.043	0.086
E_{Kin}	0.075	0.060	0.000	0.006	0.005
$E_{Ion\text{-}Ion}$	0.058	0.043	0.006	0.000	0.008
number	0.106	0.086	0.005	0.008	0.000

S.5.2 Orthogonal tests

Optimal conditions can be obtained after the orthogonal tests and subsequent data analysis. In this section, the simulations were based on an orthogonal array experimental design (L_9 matrix) where the following three variables of laser were analyzed: intensity (factor A), wavelength (factor

B), and pulse duration (factor C). These variables were identified to have great effects on the degree of photodissociation of phenol from corresponding simulations proceeded above. An L_9 (3^4) matrix, which is an orthogonal array of three factors and three levels, was employed to assign the considered factors and levels as shown in Table S12.

Table S12 Levels and factors affecting the photodissociation of phenol.

Level	Factors		
	A-Intensity (W/cm^2)	B-Wavelength (nm)	C-Duration (fs)
1	7	400	10
2	8	600	20
3	9	800	40

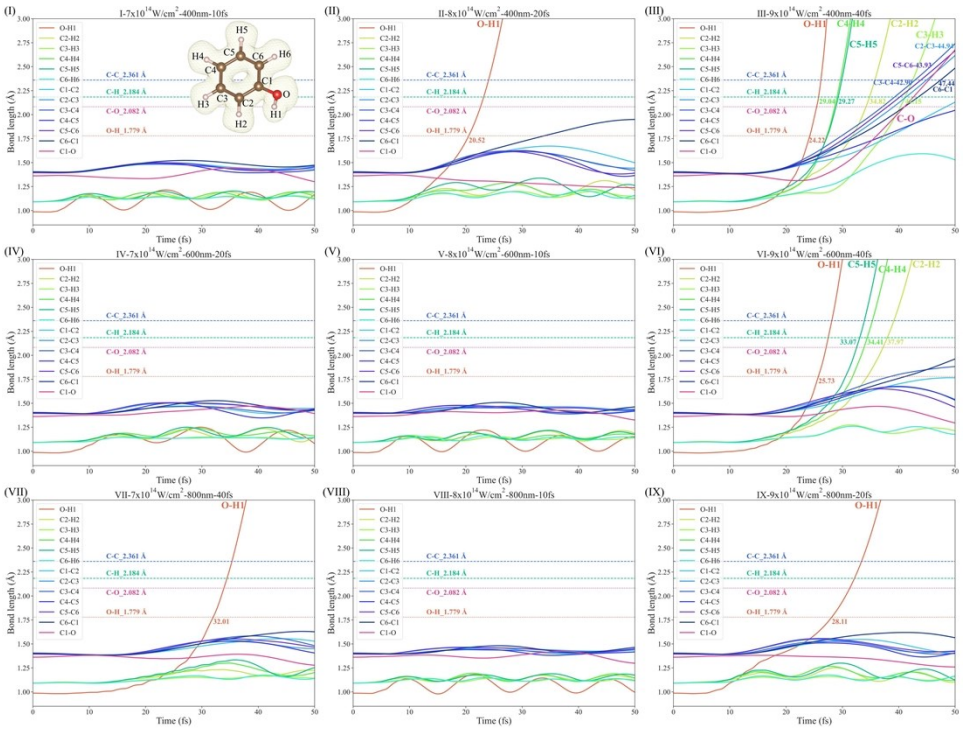

Figure S7 Time evolution of bond lengths of laser-induced phenol photodissociation dynamics in L_9 tests. The red, pink, green and blue horizontal dotted lines respectively indicate the critical value of O-H1, C1-O, C-Hs and C-Cs.

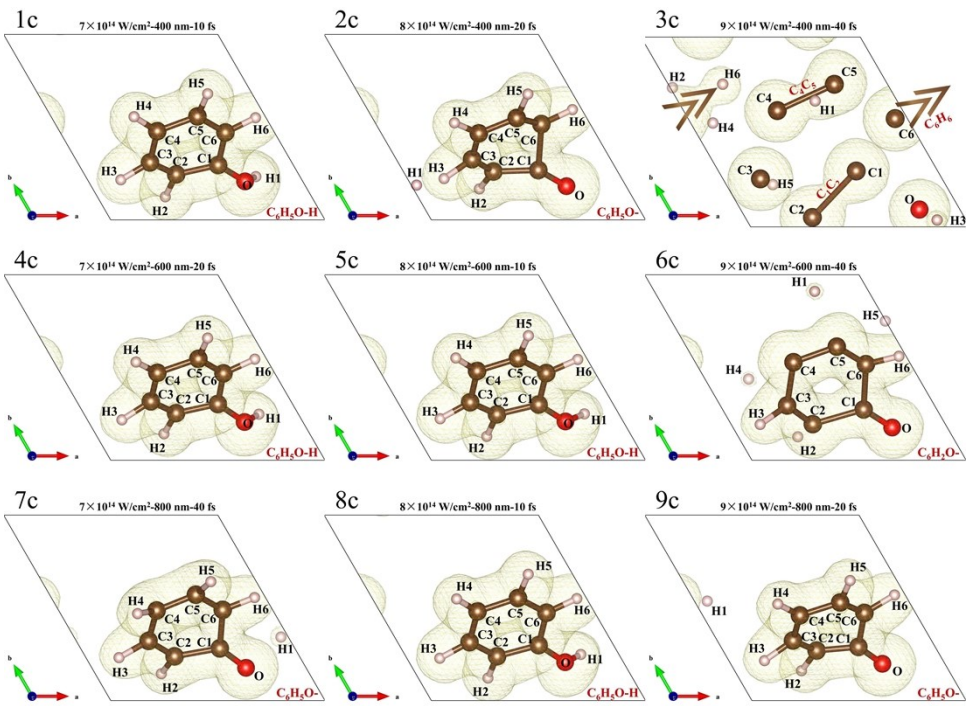

Figure S8 Final ELF patterns of an isolated phenol under the various pulse lasers in the L_9 tests (xy-plane)

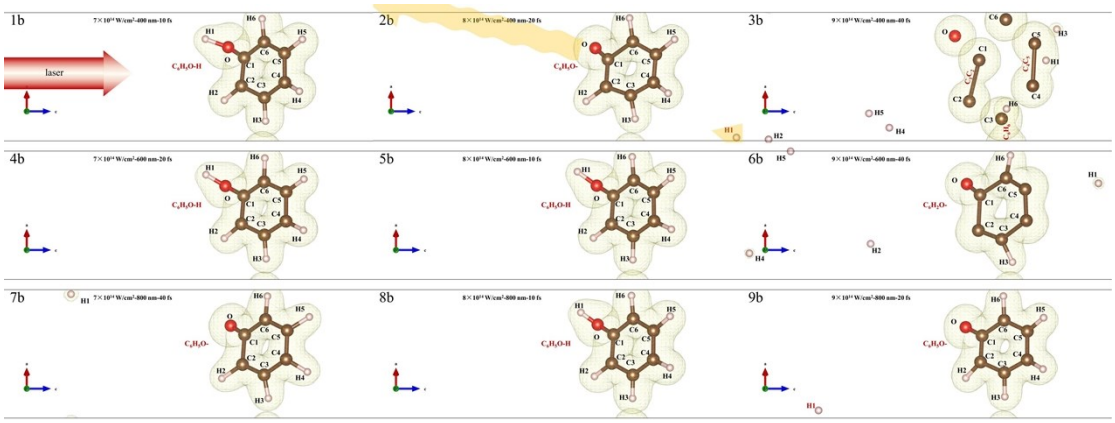

Figure S9 Final ELF patterns of an isolated phenol under various pulse lasers in the L_9 tests (xz-plane)

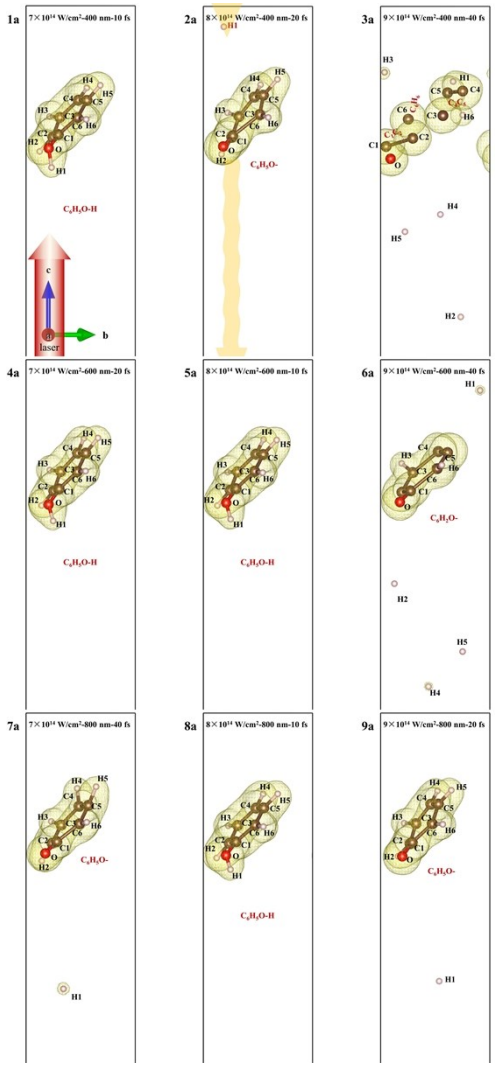

Figure S10 Final ELF patterns of an isolated phenol under various pulse lasers in the L_9 tests (yz-plane)

Nine trials were carried out according to the L_9 matrix; each row of orthogonal array represents a run. The results obtained from the preliminary analysis of photodissociation dynamics are set out in Figure S8-10. From the third experiment, the one of complete dissociation of phenol, the critical values for C-C bond (2.361 Å) and C-O bond (2.082 Å) can be estimated, and the following bond cleavage sequence can be obtained: 1st: O-H1, 2nd: C5-H5, 3rd: C4-H4, 4th: C2-H2, 5th: C1-O, 6th:C3-H3, 7th:C3-C4, 8th: C5-C6, 9th:C2-C3, 10th: C6-C1. The generated free radicals have the ability to transform into all the products (1,4-Dihydroxybenzen, 1,2-Benzenediol, 1,4-Benzoquinone and cis-2-Butenedioic acid) currently detected in experiments. According to our results in the former sections and others', hydrogen detachment or transfer should be concerned in a photodissociation of phenol majorly mainly[3]. Therefore, we consider the case where only the O-H is decomposed as the highest score, and the score is reduced accordingly when multiple bonds are dissociated. If

the molecule is not dissociated, the greater the vibration amplitude, set the score higher. Further data analysis was carried out through the range analysis and analysis of variance to reflect the optimal laser conditions and their magnitudes. K_{ji} and R_j are two important parameters in a range analysis. K_{ji} is the sum of the evaluation indexes of all levels (i, i = 1, 2, 3) in each factor (j, j = A, B, C) and k_{ji} (mean value of K_{ji}) is employed to estimate the optimal level and the optimal combination of factors. The optimal level for each factor could be obtained when k_{ji} is the largest. R_j is defined as the range between the maximum and minimum value of k_{ji} to evaluate the importance of the factors, i.e., a larger R_j means a greater importance of the factor. For instance, take this L_9 (3^4) matrix. The calculation is shown as following:

For the factor of A:

$$K_{A1} = D_1 + D_4 + D_7$$

$$K_{A2} = D_2 + D_5 + D_8$$

$$K_{A3} = D_3 + D_6 + D_9$$

$$k_{A1} = \frac{K_{A1}}{3}; k_{A2} = \frac{K_{A2}}{3}; k_{A3} = \frac{K_{A3}}{3}$$

$$R_j = k_{ji}(max) - k_{ji}(min)$$

Table S13 Visual analysis table of L_9 tests for laser-induced photodissociation of phenol

Tests No.	Factors					
	A-intensity (W/cm^2)		B-wavelength (nm)		C-time (fs)	D-degree
1	7		400		10	52
2	8		400		20	100
3	9		400		40	59
4	7		600		20	60
5	8		600		10	53
6	9		600		40	83
7	7		800		40	90
8	8		800		10	48
9	9		800		20	95
K_{Ai}	K_{A1}	202	K_{A2}	201	K_{A3}	237
K_{Bi}	K_{B1}	211	K_{B2}	196	K_{B3}	233
K_{Ci}	K_{C1}	153	K_{C2}	255	K_{C3}	232

k_{Ai}	k_{a1}	67.33	k_{a2}	67	k_{a3}	79
k_{Bi}	k_{b1}	70.33	k_{b2}	65.33	k_{b3}	77.67
k_{Ci}	k_{c1}	51	k_{c2}	85	k_{c3}	77.33
R_j	R_A	12	R_B	12.34	R_C	34
Primary order			$R_C > R_B > R_A$			
Superior level		A3		B3		C2
Superior Combination			A3B3C2=9×10^{14}W/cm^2-800 nm-20fs			

Table S13 is the visual analysis table of the orthogonal tests of laser-induced dissociation of phenol. It can be seen from the table that $R_C > R_B > R_A$, indicating that the order of the influence of various factors on the dissociation of phenol is: pulse duration >wavelength> peak intensity. Therefore, the optimal laser conditions for inducing the dissociation of phenol are: 9×10^{14}W/cm^2-800 nm-20 fs. It also should be concluded that, for an isolated phenol, the 1st cleavage bond is O-H1, no matter what the laser parameters are, which is consist with the observation in the H atom elimination experiment[4].

S.5.3 The photodissociation of phenol absorbed over a perfect 2D g-C_3N_4 sheet

Graphitic carbon nitride (g-C_3N_4) is typical adsorbent employed in the process of photocatalytic experiments widely[5]. Besides 2D graphene, here we also have built the adsorption models of a phenol molecule adsorbed over a perfect 2D g-C_3N_4 sheet to simulate the photodissociation mechanism of an adsorbed phenol molecule and the details of the model building are discussed in the 'S.1' subsections of the Supplemental Material. As mentioned above, we marked the phenomenon that electrons do not locate the bond around as a reliable prediction of photodissociation of phenol molecule. One finding that emerged from the Figure S11 is, with the laser being 800 nm and pulse duration time lasting for 40fs, the adsorbed phenol molecule over a perfect 2D g-C_3N_4 sheet started to dissociate when the intensity was 4×10^{14}W/cm^2. That means while the phenol molecule is adsorbed over a g-C_3N_4 sheet, the intensity threshold is reduced to 4×10^{14}W/cm^2, which is about a half diminution with respect to the isolated one (with laser being

800 nm-40 fs). That may be attributed to E-field enhancement of a 2D graphite material[6].

And the other finding is that the 1st bond dissociated in such condition is the C5-H5 bond (occupying the anti-meta-position) rather than the O-H and the products are a H fragment dissociated from it and a $-C_6H_4OH$ radical. The details of the time evolution of the ELFs for this adsorbed model under the laser 4×10^{14} W/cm^2-800 nm-40 fs in Figure S11 also proved it. This is a similar phenomenon that was found in the condition in clusters with suppressing effect[7]. The results of this paper show that the cleavage of the bonds of phenol is not simultaneous but sequential; O-H1 is the most vulnerable bond in an isolated phenol molecule, and that in an adsorbed phenol molecule is C-H.

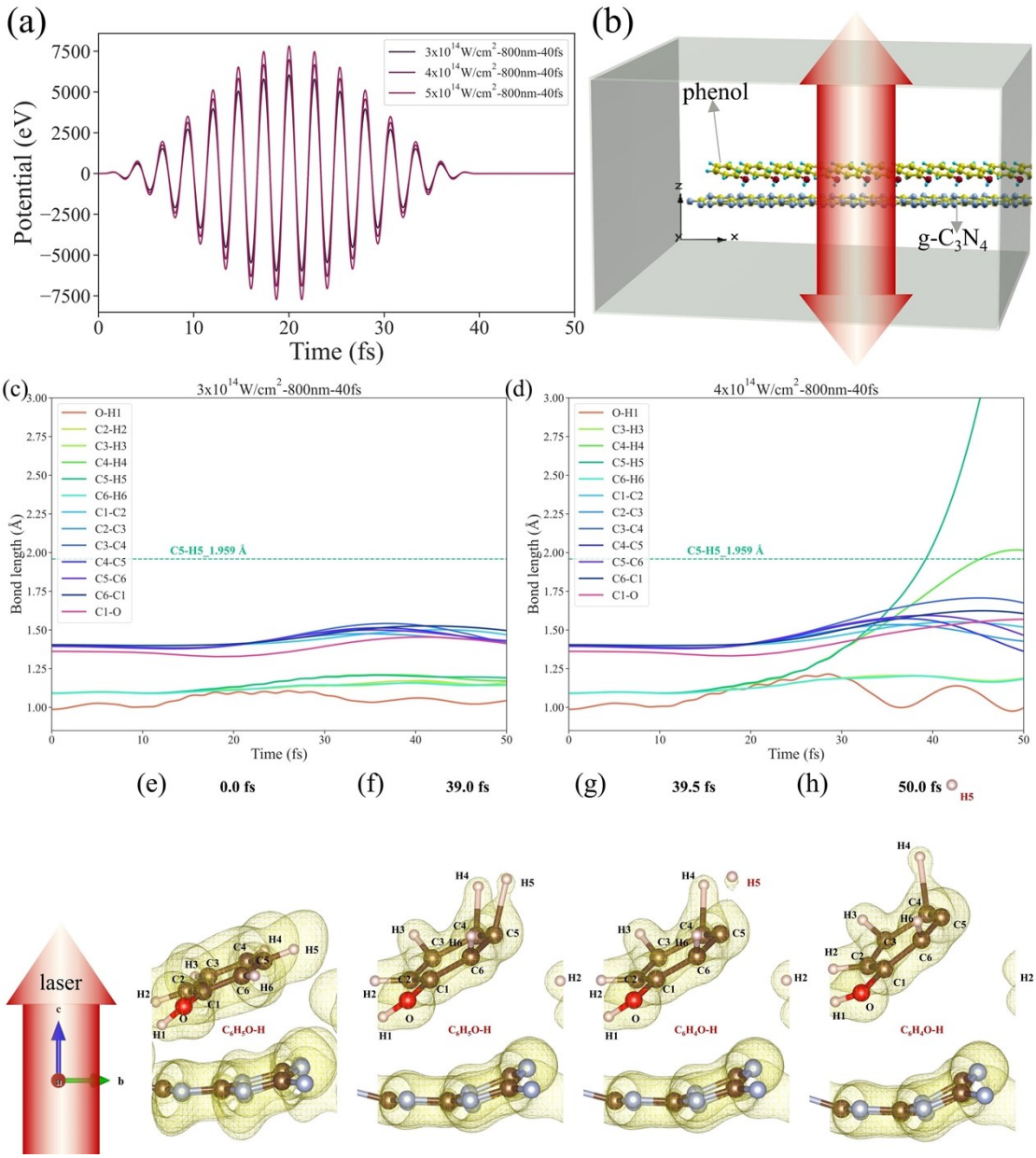

Figure S11 (a) Profile of applied laser pulses with peak intensity I = 3 × 10^{14}W/cm^2 to I = 5 × 10^{14}W/cm^2. (b) Schematic explaining the polarization vector (red arrow, which is along z-axis and perpendicular to a 2D sheet) of the incident laser beam for the g-C_3N_4 nanosheet with phenol molecules. The middle three panels show the time evolution of the bond lengths of the phenol under the pulse laser with intensity being (c) 3×10^{14}W/cm^2 (d) 4×10^{14}W/cm^2 (e) 5×10^{14}W/cm^2. Various bonds are colored by order (red: O-H; green series: C-Hs; blue series: C-Cs; pink: C-O). The corresponding dotted lines locate the bond length when O-H and C-Hs realize the fracture. The below four snapshots show the ELF patterns of an adsorbed phenol under the 4×10^{14}W/cm^2-800 nm-40fs pulse laser over perfect 2D g-C_3N_4 sheet at (f) 0.0 fs, (g) 39.0 fs, (h) 39.5 fs and (i) 50 fs.

[1] Octopus, Tutorial:Total energy convergence, in: https://octopus-code.org/wiki/Tutorial:Total_energy_convergence, 2018.
[2] T.S. K. Yabana, Y. Shinohara, T. Otobe, and G.F. Bertsch, Time-dependent density functional theory for strong electromagnetic fields in crystalline solids, Phys. Rev. B: Condens. Matter, 85 (2012) 045134.
[3] G.A. Pino, A.N. Oldani, E. Marceca, M. Fujii, S.I. Ishiuchi, M. Miyazaki, M. Broquier, C. Dedonder, C. Jouvet, Excited state hydrogen transfer dynamics in substituted phenols and their complexes with ammonia: pipi*-pisigma* energy gap propensity and ortho-substitution effect, J. Chem. Phys., 133 (2010) 124313.
[4] C.M. Tseng, Y.T. Lee, C.K. Ni, H atom elimination from the pi sigma* state in the photodissociation of phenol, J. Chem. Phys., 121 (2004) 2459-2461.
[5] X. Chen, J. Zhang, X. Fu, M. Antonietti, X. Wang, Fe-g-C_3N_4-Catalyzed Oxidation of Benzene to Phenol Using Hydrogen Peroxide and Visible Light, J. Am. Chem. Soc., 131 (2009) 11658–11659.
[6] Y. Miyamoto, H. Zhang, X. Cheng, A. Rubio, Modeling of laser-pulse induced water decomposition on two-dimensional materials by simulations based on time-dependent density functional theory, Phys. Rev. B: Condens. Matter, 96 (2017) 115451.
[7] V. Poterya, L. Sistik, P. Slavicek, M. Farnik, Hydrogen bond dynamics in the excited states: photodissociation of phenol in clusters, Phys. Chem. Chem. Phys., 14 (2012) 8936-8944.